

# Procedure to Calculate the Inductance of a Circular Loop Near a Metal Plate

**Abstract.** This paper describes the influence of metallic objects on the inductance as a function of the separation distance. We focus our attention on the benchmark configuration of a circular loop antenna near an infinite conducting plate. We consider the quasi-static approach, thus with a constant current distribution over the entire loop. The results are obtained by numerical integration and the accuracy of the numerical integration procedure is verified for a circular loop antenna in free space, for which a closed analytical solution exists. The results are particularly interesting in the domain of low frequency and high frequency Radio Frequency IDentification, where mutual influence of multiple reader antennas is often suppressed by means of a metallic shielding, which results in an important decrease of the readout distance and a detuning of every reader antenna.

**Abstract.** W artykule opisano wpływ obiektów metalowych na indukcyjność jako funkcję dystansu. Analizowano okrągłą antenę w pobliżu nieskończoności długiej metalowej płytki. Badania mają znaczenie w układach RFID gdzie liczne anteny są zakrywane przez metalowe ekranie. (Analiza indukcyjności okrągłej anteny w pobliżu metalowej płyty)

**Keywords:** circular loop, inductance, RFID.

**Słowa kluczowe:** antena RFID, indukcyjność.

## 1. Introduction

The inductance  $L$  of a circular loop at low frequencies in free space is well described in the literature [1]. In practice though, objects close to the inductive element can have an important influence. This is especially true for metals and conductive bodies in general, where the induced voltage leads to a current that gives rise to a flux that opposes the change in flux (Lenz's law, see [2]).

For Radio Frequency IDentification (RFID) systems, the modification of the  $L$  is crucial, since it is an indicator for the volume in which a tag can be read.

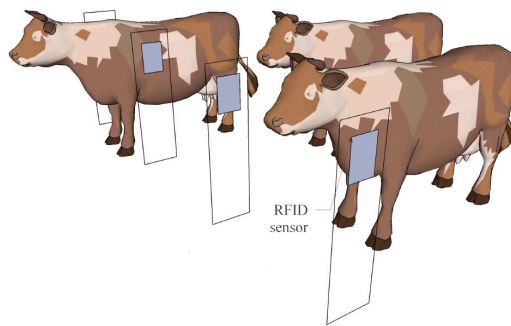


Fig. 1. Illustration of a setup with cows in parallel lines.

In certain RFID configurations, it is important that the reader antenna only detects that tag that is meant to be read, and not one that is only slightly further away. An example is an automatic feeding installation in the cattle industry. The goal is to automatically link the amount of food with every individual animal. RFID is an excellent technology for this, since it is an automatic contact-less identification method that supports well possible dirt or moisture. Often, RFID installations are close to each other so there is a chance that not only the animal in that specific feeding box or transfer line is detected, but also the one in the line nearby. This is illustrated in Fig. 1. Processing these data can thus lead to conflicts. This is obviously an electromagnetic compatibility issue: two or more devices hinder the correct operation of one another due to their electromagnetic proximity. A simple solution for this problem is the usage of metallic screens between the boxes. Fig. 1. Illustration of a setup with cows in parallel

lines. This configuration blocks the field of one reader antenna to penetrate a neighboring box, thus avoiding the readout of the tag in that box. Care must be taken when installing these shielding metals, since one still wants the reader antenna to read the tag that is in the box to be read. Another issue is that as the inductance is modified, the circuit of the reader becomes detuned.

In this paper, we will develop a numerical procedure to determine the decrease of the inductance  $L$  of a circular loop as a function of the distance from a perfectly conducting plate.

## 2. Inductance of a loop

### A. Formulation

For lower frequencies, the Biot-Savart law may be applied for the calculation of the magnetic field caused by a known current distribution.

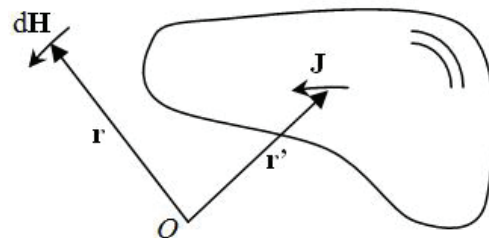


Fig. 2. Biot-Savart law: Conventions with regard to equation (1).

Using the conventions of Fig. 2, the equation (1) is valid for a known volume current flowing within an elementary volume  $dV$  [2]. We consider non-magnetic materials ( $\mu_r = 1$ ) for the rest of this paper.

$$(1) \quad d\mathbf{H}(\mathbf{r}, \mathbf{r}') = \frac{1}{4\pi} \frac{[\mathbf{J}(\mathbf{r}')dV] \times (\mathbf{r} - \mathbf{r}')}{|\mathbf{r} - \mathbf{r}'|^3}$$

For surface (in case of perfect electrical conductors) or line currents, respectively equations (2) and (3) can be applied [2]. In equation (2),  $\mathbf{K}(\mathbf{r}0)$  is a surface current, while in equation (3),  $\mathbf{dl}(r0)$  is an elementary line current.

$$(2) \quad d\mathbf{H}(\mathbf{r}, \mathbf{r}') = \frac{1}{4\pi} \frac{[\mathbf{K}(\mathbf{r}')dS] \times (\mathbf{r} - \mathbf{r}')}{|\mathbf{r} - \mathbf{r}'|^3}$$

$$(3) \quad d\mathbf{H}(\mathbf{r}, \mathbf{r}') = \frac{1}{4\pi} \frac{dI(\mathbf{r}') \times (\mathbf{r} - \mathbf{r}')}{|\mathbf{r} - \mathbf{r}'|^3}$$

If the size of the wire is small with regard to the wavelength, one may consider the magnitude of the current  $I$  constant along the wire:  $dI(r') = Idl(r')$ . This leads to equation (4), where  $dl(r')$  is an elementary segment length along the wire in the direction of the current (see Fig. 3). Due to the superposition principle, the total magnetic field  $\mathbf{H}(r)$  can thus be written as in equation (5) ( $L_w$  is the total length of the wire).

$$(4) \quad d\mathbf{H}(\mathbf{r}, \mathbf{r}') = \frac{I}{4\pi} \frac{dl(\mathbf{r}') \times (\mathbf{r} - \mathbf{r}')}{|\mathbf{r} - \mathbf{r}'|^3}$$

$$d\mathbf{H}(\mathbf{r}, \mathbf{r}') = \frac{I}{4\pi} \frac{dl(\mathbf{r}') \times (\mathbf{r} - \mathbf{r}')}{|\mathbf{r} - \mathbf{r}'|^3}$$

$$(5) \quad \mathbf{H}(\mathbf{r}) = \frac{I}{4\pi} \int_{L_w} \frac{dl(\mathbf{r}') \times (\mathbf{r} - \mathbf{r}')}{|\mathbf{r} - \mathbf{r}'|^3}$$

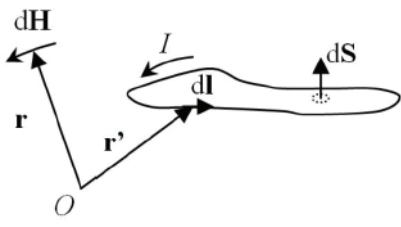


Fig. 3. The Biot-Savart law in case of a line current.

In order to calculate the inductance  $L$  of a loop antenna, one must determine the total amount of flux. The flux is defined as in equation (6) [2], with  $S_l$  the total inner surface enclosed by the loop. Once the total amount of flux is known, it is easy to calculate the inductance  $L$  using equation (7).

$$(6) \quad \Phi = \mu_0 \int_{S_l} \mathbf{H}(\mathbf{r}) \cdot d\mathbf{S}$$

$$(7) \quad L = \frac{\Phi}{I}$$

#### B. Inductance of a circular loop in free space

Consider Figure 4. The circular loop has a wire radius of  $r_w$  and the distance from the origin  $O$  to the centre of the wire is called  $r_l$ , the loop radius. Based on rotational symmetry and symmetry with regard to the  $xy$ -plane, one can see that knowledge of the magnetic field in the first quadrant of the  $yz$ -plane is sufficient to know the field anywhere else. For most practical applications, the radius of the wire  $r_w$  is much smaller than  $r_w$ . Generally, at low frequencies, when the wire has a finite conductivity, a volume current will be distributed over the dashed area of Fig. 4. If one wants to calculate this rigorously, one has to apply equation (1). It is clear that this is a complicated task. Let us suppose that there is an equivalent line current  $I$  flowing on a curve in the centre of the circular wire, defined by equation (8), where  $\mathbf{J}$  represents the current density flowing through the dashed area of Figure 4. This choice is justified by using the integral representation of Ampère's law. This is valid of course as long that we do not try to calculate the magnetic field inside the wire. This approach facilitates the calculations significantly.

$$(8) \quad I = \int_{S_w} \mathbf{J}(\mathbf{r}') \cdot d\mathbf{S}(\mathbf{r}')$$

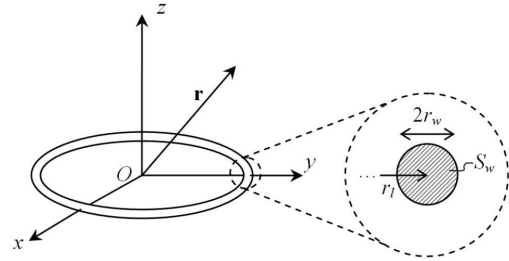


Fig. 4. Circular current loop in free space.

Due to symmetry reasons and the fact that we have chosen the  $yz$ -plane as the observation plane, a mixture of cylindrical (for the excitation location  $\mathbf{r}'$ ) and cartesian coordinates (for the observation location  $\mathbf{r}$ ) are the most convenient to handle the configuration of Fig. 4. For the application of equation (5), it is clear that  $dl(r')$  equals  $r_l d\phi' \mathbf{u}_{\phi'}$ , with  $\mathbf{u}_{\phi'}$  the unit vector in the  $\phi'$ -direction. Our equivalent line current is thus flowing counterclockwise in the  $xy$ -plane. After some elementary mathematical manipulations, one obtains the following components of the magnetic field as in equations (9), (10) and (11) in the  $yz$ -plane.

$$(9) \quad H_x(y, z) = \frac{Ir_l z}{4\pi} \int_0^{2\pi} \frac{\cos \phi' d\phi'}{(r_l^2 + y^2 - 2r_l y \sin \phi' + z^2)^{3/2}}$$

$$(10) \quad H_y(y, z) = \frac{Ir_l z}{4\pi} \int_0^{2\pi} \frac{\sin \phi' d\phi'}{(r_l^2 + y^2 - 2r_l y \sin \phi' + z^2)^{3/2}}$$

$$(11) \quad H_z(y, z) = \frac{Ir_l}{4\pi} \int_0^{2\pi} \frac{(r_l - y \sin \phi') d\phi'}{(r_l^2 + y^2 - 2r_l y \sin \phi' + z^2)^{3/2}}$$

These integrals cannot be solved analytically. After numerical calculation of  $H_x(y, z)$  (equation (9)), this component seems to be zero for all values of  $y$  and  $z$ . Remember that these equations are valid in the  $yz$ -plane, but that due to symmetry, they are sufficient to know the field at any other place. This means that the magnetic field of a circular loop has no  $\phi$  component (expressed in cylindrical coordinates), but only a vertical and radial contribution. Expressing the field in cylindrical components results in equations (12), (13) and (14).

$$(12) \quad H_\phi(r, z) = 0$$

$$(13) \quad H_r(r, z) = \frac{Ir_l z}{4\pi} \int_0^{2\pi} \frac{\sin \phi' d\phi'}{(r_l^2 + r^2 - 2r_l r \sin \phi' + z^2)^{3/2}}$$

$$(14) \quad H_z(r, z) = \frac{Ir_l}{4\pi} \int_0^{2\pi} \frac{(r_l - r \sin \phi') d\phi'}{(r_l^2 + r^2 - 2r_l r \sin \phi' + z^2)^{3/2}}$$

On the  $z$ -axis, we have thus  $H_z(0, z) = 0$  and equation (15), which is a well-known result. Remark also that in the  $xy$ -plane, there is only a vertical component of the magnetic field.

$$(15) \quad H_z(0, z) = \frac{I}{2} \frac{r_l^2}{(r_l^2 + z^2)^{3/2}}$$

For the calculation of the inductance  $L$ , one has to evaluate the integral of equation (6). For our circular loop antenna in free space, this leads to equation (16). Knowledge of  $H_z(r,0)$  is crucial for the numerical determination of the flux  $\Phi$ . In order to have an idea of  $H_z(r,0)$ , let us focus the attention on an example with typical dimensions, namely  $r_l = 0.15 \text{ m}$  and  $S_w = 1.5 \text{ mm}^2$ .  $1.5 \text{ mm}^2$  is the cross section surface of a wire typically used for low power electrical installations (e.g., power lines for lighting), and thus a standard dimension. The result is shown on Fig. 5. The equivalent line current  $I$  is normalized to  $1 \text{ A}$ , which is also the case for the other field plots in this paper.

$$(16) \quad \Phi = 2\pi\mu_0 \int_0^{r_l-r_w} H_z(r,0) r dr$$

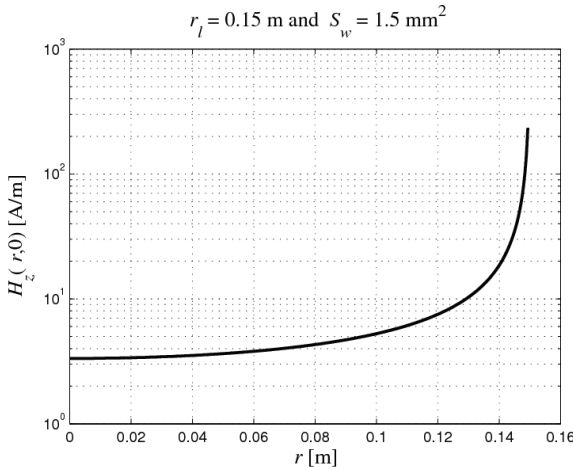


Fig. 5. Characteristic radial variation of the vertical magnetic field within the loop.

It is clear that the numerical integration of  $H_z(r,0)$ -values close to  $r_l - r_w$  requires dense sampling. With standard numerical integration techniques (e.g., Simpson's rule), we obtain a value of  $L$ . In this specific example, we have a value of  $1.029109 \mu\text{H}$ . In order to verify the accuracy of this result, we have compared this with a formula that is available [1], namely equation (17). Application for our specific example of the closed form (17) leads to an inductance of  $1.029131 \mu\text{H}$ , or a relative deviation of less than 0.003 % with regard to our numerical procedure. We have verified our approach compared to  $L_{\text{analytical}}$  for numerous other loop dimensions and wire diameters and the correctness of our method was confirmed.

$$(17) \quad L_{\text{analytical}} = \mu_0 r_l \left[ \ln\left(\frac{8r_l}{r_w}\right) - 2 \right]$$

One can ask why doing all the bother if calculation of (17) leads rapidly to a good result. We have used  $L_{\text{analytical}}$  as a verification of our method. In the next section, we will apply the same methodology for a configuration for which no simple closed-form analytical expression is available, namely a conductor loop close to a metallic plate.

#### C. Inductance of a circular loop near a metal plate

Consider Fig. 6. It shows our current loop close to a perfectly conducting plate of infinite transversal dimensions, located at the plane  $z = -d$ . We know that the magnetic field at the plane  $z = -d$  must be tangential. For  $z \geq -d$ , the

configuration shown on Fig. 7 yields the same solution [2]. Based on superposition, we can write that for  $z \geq -d$ , equations (18), (19) and (20) are valid.

$$(18) \quad H_\phi(r,z) = 0$$

$$H_r(r,z) = \frac{Ir_l z}{4\pi} \left[ \int_0^{2\pi} \frac{\sin \phi' d\phi'}{(r_l^2 + r^2 - 2r_l r \sin \phi' + z^2)^{3/2}} - \int_0^{2\pi} \frac{\sin \phi' d\phi'}{(r_l^2 + r^2 - 2r_l r \sin \phi' + (z + 2d)^2)^{3/2}} \right]$$

$$(19)$$

$$(20) \quad H_z(r,z) = \frac{Ir_l}{4\pi} \left[ \int_0^{2\pi} \frac{(r_l - r \sin \phi') d\phi'}{(r_l^2 + r^2 - 2r_l r \sin \phi' + z^2)^{3/2}} - \int_0^{2\pi} \frac{(r_l - r \sin \phi') d\phi'}{(r_l^2 + r^2 - 2r_l r \sin \phi' + (z + 2d)^2)^{3/2}} \right]$$

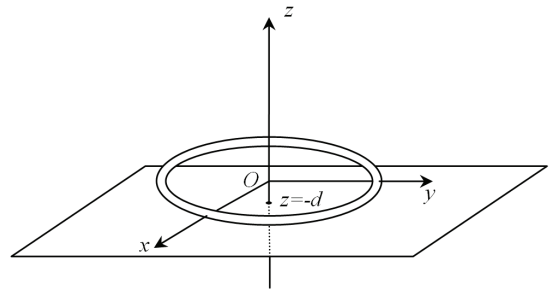


Fig. 6. Circular current loop near a metal plate.

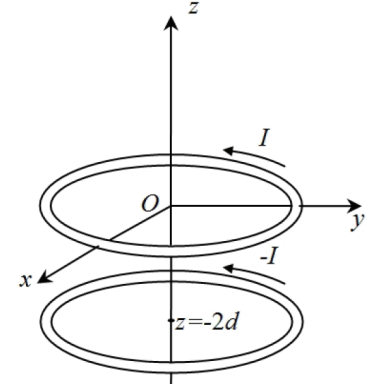


Fig. 7. Introduction of the image current.

For different distances  $d$ , we can calculate the inductance  $L$ , using the same numerical procedure we applied for the circular loop in free space. It is clear that as  $d$  becomes small, the field is decreasing, especially for larger values of  $z$ . For the evaluation of the flux, it is especially the vertical magnetic field in the  $xy$ -plane that has to be determined. Let us consider the same loop parameters as before ( $r_l = 0.15 \text{ m}$  and  $S_w = 1.5 \text{ mm}^2$ ) at a distance  $d$  of  $1 \text{ cm}$ . In Fig. 8, the vertical magnetic field distribution in the  $xy$ -plane is plotted in free space and for a separation distance  $d$  of  $1 \text{ cm}$ . Close to the wire, the equivalent line current dominates, and thus the two curves coincide. In the centre of the loop though, the field values differ in more than an order of magnitude. It is thus obvious that the inductance  $L$  will decrease significantly as the loop is nearing the metal plate. For these specific loop

parameters, you can find the variation of  $L$  as  $d$  changes on Fig. 9. We have plotted the ratio  $L_d/L_\infty$ , where  $L_d$  stands for the inductance at a certain distance from the plate  $d$ .  $L_\infty$  represents the inductance in free space, which is  $1.0291 \mu\text{H}$ . From this figure and thus for this specific example, one can clearly see that as the distance between the plate and the loop antenna becomes smaller than a couple of cm's, that  $L_d$  drops rapidly and that the reader antennae circuit will be detuned.

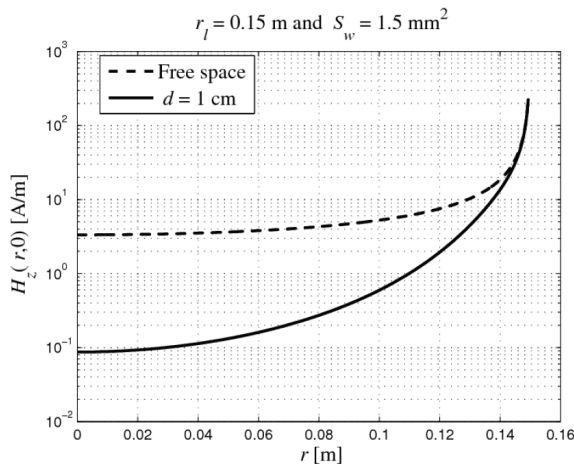


Fig. 8. Characteristic radial variation of the vertical magnetic field within the loop in free space and for  $d = 1 \text{ cm}$ .

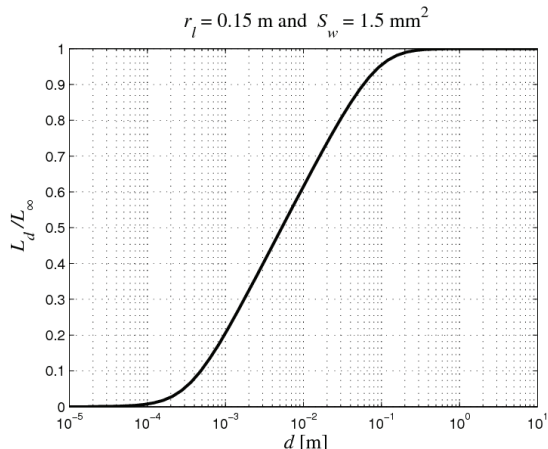


Fig. 9. Variation of  $L_d/L_\infty$  as a function of  $d$ .

### 3. Conclusion

In this paper, we have developed a numerical procedure to determine the magnetic field generated by a circular loop in free space or close to a metal plane. The method has been verified by means of the inductance  $L$ , which is known for a circular loop antenna in free space. Based on this procedure and the principle of superposition, one can generate a large amount of theoretical predictive models how circular loops will behave when they are surrounded by metal objects.

This is especially interesting for the usage of metals as screening shields in the domain of RFID. We have quantified for an example how an RFID loop antennae is detuned as the distance between the metal plane and the reader decreases. This effect, together with the weakened magnetic field, can make that a reader antenna is not capable to detect tags anymore if no special precautions are taken.

### REFERENCES

- [1] F. W. Grover, Inductance Calculations: Working Formulas and Tables, New York: Dover, 1946.
- [2] D. J. Griffiths, Introduction to Electrodynamics, Englewood Cliffs, New Jersey: Prentice Hall, 1981.

### Authors.

Nobby Stevens, Catholic University College Gent, Association K.U.Leuven, DraMCo research group, Gebr. Desmetstraat 1, Gent, Belgium, Email: [nobby.stevens@kahosl.be](mailto:nobby.stevens@kahosl.be)  
 Lieven Destrycker, Catholic University College Gent, Association K.U.Leuven, DraMCo research group, Gebr. Desmetstraat 1, Gent, Belgium , Email: [lieven.destrycker@kahosl.be](mailto:lieven.destrycker@kahosl.be)  
 Werner Verschelde, Catholic University College Gent, Association K.U.Leuven, Gebr. Desmetstraat 1, Gent, Belgium, Email: [werner.verschelde@kahosl.be](mailto:werner.verschelde@kahosl.be)